

The Standard RV Equation uses ω_p , not ω_*

AARON HOUSEHOLDER ¹ AND LAUREN WEISS ²

¹ *Yale University, 52 Hillhouse, New Haven, CT 06511, USA*

² *Department of Physics and Astronomy, University of Notre Dame, Notre Dame, IN 46556, USA*

ABSTRACT

Since the discovery of the first exoplanet orbiting a main-sequence star, astronomers have used stellar radial velocity (RV) measurements to infer the orbital properties of planets. For a star orbited by a single planet, the stellar orbit is a dilation and 180° rotation of the planetary orbit. Many of the orbital properties of the star are identical to those of the planet including the orbital period, eccentricity, inclination, longitude of the ascending node, time of periastron passage, and mean anomaly. There is a notable exception to this pattern: the argument of periastron, ω , which is defined as the angle between the periapsis of an orbiting body and its ascending node; in other words, ω describes the orientation of a body’s elliptical path within the orbital plane. For a star-planet system, the argument of periastron of the star (ω_*) is 180° offset from the argument of periastron of the planet (ω_p). For a conventional coordinate system with \hat{z} pointed away from the observer, the standard RV equation is defined with ω_p ; however, we find that many interpretations of the RV equation are not self-consistent. For instance, the commonly used Radial Velocity Modeling Toolkit **RadVel** relies on an RV equation that uses the standard ω_p , but its documentation states that it instead models ω_* . As a result, we identify 54 published papers reporting a total of 265 ω values that are likely 180° offset from their true values, and the scope of this issue is potentially even larger.

1. INTRODUCTION

The radial velocity (RV) method is one of the most common ways to detect and characterize exoplanets. According to the NASA Exoplanet Archive (accessed 2022 Nov 07), the RV method is responsible for the characterization of nearly 2000 exoplanets (Akeson et al. 2013). The RV method works by measuring the Doppler shift in the spectral features of a star, which allows us to determine changes in the star’s line of sight velocity caused by the gravitational influence of orbiting planets. This technique gives us information about planetary masses as well as the orbital properties of the planet and its host star.

There are several publicly available tools that forward model orbital elements from RV measurements, including the widely used Radial Velocity Modeling Toolkit **RadVel** (Fulton et al. 2018). When modeling RVs, we must model the argument of periastron, ω , which is defined as the angle between the ascending node and the periapsis of a body’s orbit. For a star-planet system the argument of periastron of the star (ω_*) is 180° offset from the argument of periastron of the planet (ω_p). We noticed that **RadVel** produces values for ω_* that are consistent with values of ω_p in other packages such as **TTVFast** (Deck et al. 2014). In section 2, we describe the

RadVel RV model and its underlying equations that use ω . We also assess this parameterization of ω in **RadVel** using a first principles approach and compare the results to **TTVFast**.

2. MODELING RVs WITH RADVEL

RadVel gives users the tools to fit Keplerian orbits to RV measurements by using the Markov Chain Monte Carlo (MCMC) method within **emcee** (Foreman-Mackey et al. 2013). RV orbits are described with five orbital elements. These parameters are the orbital period (P), time of periastron passage (t_p), eccentricity (e), the argument of periastron of the star (ω_*), and the RV semi-amplitude (K).

RadVel generates RVs by solving the following system of equations (1-3):

$$M = E - e \sin E \quad (1)$$

$$\nu = 2 \tan^{-1} \left(\sqrt{\frac{1+e}{1-e}} \tan \frac{E}{2} \right) \quad (2)$$

$$v_r = \dot{z} = K [\cos(\nu + \omega_*) + e \cos(\omega_*)] \quad (3)$$

where M is the mean anomaly, E is the eccentric anomaly, e is the orbital eccentricity, ν is the true

anomaly, v_r is the stellar RV induced by an orbiting planet, K is the RV semi-amplitude, and ω_* is the argument of periastron of the star.

Equation 3 in **RadVel** uses ω_* , rather than the standard ω_p , for an important reason: coordinate system selection. We present evidence, however, that the current **RadVel** coordinate system is inverted, which manifests as an issue with the modeling of ω . The **RadVel** documentation states that it uses a coordinate system with a \hat{z} unit vector that points away from the observer (implying a positive stellar RV when the star moves away from the observer). However, the RV equation in **RadVel** (Equation 3) is defined with the opposite coordinate system (Lovis & Fischer 2010). In other words, Equation 3 uses a coordinate system in which \hat{z} points towards the observer. This inconsistency yields a sign error in the **RadVel** computation of RVs, which can be corrected by changing Equation 3 to the following:

$$v_r = \dot{z} = -K[\cos(\nu + \omega_*) + e \cos(\omega_*)] \quad (4)$$

Equivalently, Equation 4 can be re-written in terms of ω_p rather than ω_* (given that $\omega_* = \omega_p + 180^\circ$):

$$v_r = \dot{z} = K[\cos(\nu + \omega_p) + e \cos(\omega_p)] \quad (5)$$

Thus, the inversion of the **RadVel** coordinate system is tantamount to modeling ω_p rather than ω_* . This is not the first time that a publicly-available package has modeled the incorrect ω value (Wright & Howard 2013). The confusion regarding which ω to use in the RV equation likely stems from the commonly cited derivation of the RV equation in Lovis & Fischer (2010). This derivation (1) does not adequately describe the relationship between radial velocity and the defined coordinate system, and (2) is not explicit in defining which ω value should be used in the RV equation. Critically, for the standard convention with \hat{z} pointing away from the observer, the standard RV equation (without a negative sign as in Equation 4) is defined with ω_p rather than ω_* (as in Equation 5).

2.1. Parameterization of ω

We developed a test to determine if the parameterization of ω is correct and applied this test to **TTVFast** and **RadVel**. We built a mock star-planet system for a $107.8 M_\oplus$ planet orbiting a $1 M_\odot$ star using **TTVFast**. The orbiting planet has the following properties: $P = 10$ days, $e = 0.6$, $\omega_p = 0^\circ$ (i.e. $\omega_* = 180^\circ$), $i = 90^\circ$, the longitude of the ascending node $\Omega = 0^\circ$, and the mean anomaly $M = 0^\circ$ (i.e. the time of periastron passage $t_p = 0$). These parameters were chosen to induce a RV semi-amplitude of $K = 40 \text{ m s}^{-1}$. We generated synthetic

RVs for this simplified planetary system using **TTVFast** (see Figure 1) and confirmed the behavior of the RVs from first principles. The planet in our mock system has an argument of periastron of 0° which implies that the planet is at periastron as it crosses the reference plane and passes through the ascending node. Therefore, at $t = 0$ (recall $t_p = 0$), we expect the planet to be at pericenter moving towards the observer at maximum absolute velocity. Conversely, the star should also be at pericenter moving away from the observer at maximum absolute velocity. The standard convention is that RV is positive when the star moves away from the observer. Therefore, at $t = 0$, the star should be at maximum radial velocity. This expected behavior agrees with our synthetic stellar RVs from **TTVFast** (see Figure 1).

With this first principles approach, we can also test if the parameterization of ω in **RadVel** is correct. We used the `rv_drive` function in **RadVel** to generate synthetic RVs for an input of the following parameters: $P = 10$ days, $t_p = 0$, $e = 0.6$, $\omega_{input} = 180^\circ$ (recall the **RadVel** documentation states that $\omega_{input} = \omega_*$), and $K = 40 \text{ m s}^{-1}$. These are the same input parameters we used for **TTVFast** (Ω in **TTVFast** is a rotational angle on the projected sky plane, so it does not affect the expected RV curve). Thus, we expected to see the same behavior for the **RadVel** RVs as we did for the RVs generated by **TTVFast**. Figure 1 demonstrates that this is not the case. At $t = 0$, for the parameters listed above, **RadVel** computes a stellar RV at minimum velocity, not at maximum velocity as was expected. This confirms that ω_{input} for **RadVel** is ω_p , not ω_* . This can be further demonstrated by changing ω_{input} from 180° to 0° (see Figure 1), which yields **RadVel** RVs that exactly match the **TTVFast** RVs (with $\omega_p = 0^\circ$).

2.2. Scope of this Issue

Given that **RadVel** yields ω_p rather than ω_* , we conclude that many published values of ω are likely 180° offset from their true value. To address the scope of this issue, we cross-referenced papers that cite **RadVel** with planets on the NASA Exoplanet Archive. For a paper and a corresponding planet in that paper to be flagged as reporting an incorrect ω value, we required the following criteria: (1) the paper must cite **RadVel**, (2) the planetary system must have detectable RVs, and (3) the paper must report an argument of periastron value with non-zero upper and lower uncertainties. We found a total of 54 papers that report 265 ω values that meet these criteria. These references and the number of planets affected in each reference are summarized in Table 1. Notably, 177 planets were flagged in Rosenthal et al. (2021).

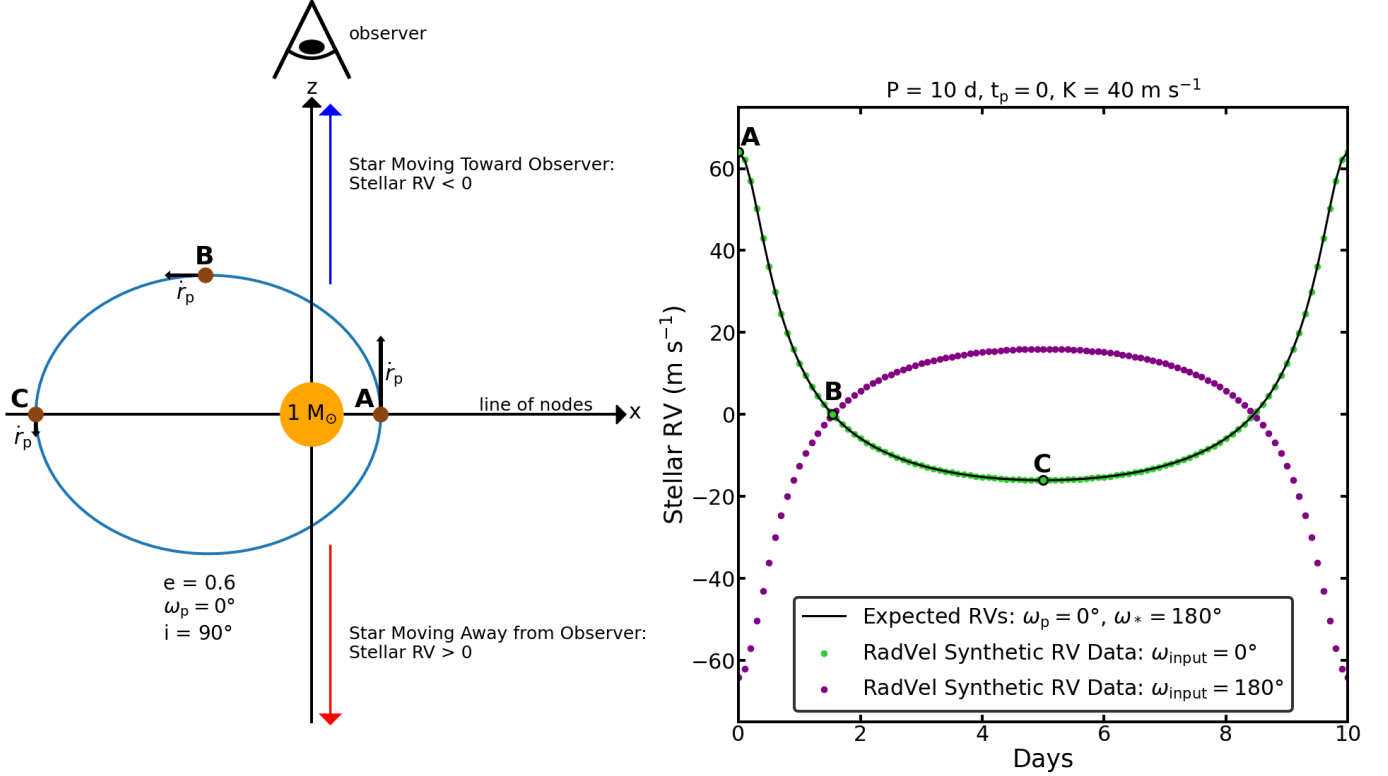


Figure 1. Left: A 2-dimensional depiction of an exoplanet (brown) orbiting a star (orange) for a simplified planetary system (adapted from Figure 7 of [Murray & Correia 2010](#)) with the following properties: $M_* = 1 M_\odot$, $P = 10$ days, $K = 40 \text{ m s}^{-1}$, $M_p = 107.8 M_\oplus$, $e = 0.6$, $\omega_p = 0^\circ$, $\omega_* = 180^\circ$, $i = 90^\circ$, $t_p = 0$, and $\Omega = 0^\circ$ (aligning the line of nodes with the x-axis). The observer is looking down from the z-axis. Labels A, B, and C correspond to three different stages of the planetary orbit. A: the planet is at periastron moving directly towards the observer, so the star is moving directly away from the observer; B: the planet and star are moving with zero radial velocity; C: the planet is at apoastron moving directly away from the observer, so the star is moving directly towards the observer. Note: stellar motion is conventionally signed negative when the star moves towards the observer and positive when the star moves away from the observer, as is denoted by the blue and red arrows. Right: The black line represents the expected radial velocity of the star from the configuration and orientation of the planetary system on the left. This line was generated with *TTVFast* and can be confirmed from first principles and the diagram on the left. The green and purple data points correspond to synthetic RVs generated by *RadVel* for $\omega_{\text{input}} = 0^\circ$ and $\omega_{\text{input}} = 180^\circ$, respectively. The *RadVel* documentation states that ω_{input} is purportedly the argument of periastron of the star (ω_*); however, the expected RVs match the green data, demonstrating that ω_{input} for *RadVel* is instead the argument of periastron of the planet (ω_p).

While our test provides a valuable gauge for the scope of this ω issue, we acknowledge that it is not a robust way to determine if a paper reports incorrect ω values. For instance, we removed [Xuan & Wyatt \(2020\)](#) from Table 1, despite the fact that it satisfied the above criteria, because the authors only cite *RadVel* to discuss their coordinate system, not to model their RV measurements. Furthermore, a significant subset of papers in Table 1 jointly modeled RVs with transits and/or transit timing variations (TTVs). We cannot easily determine how the ω issue in *RadVel* affected these papers without an in-depth analysis of each paper, which is beyond the scope of this work.

It is also possible that some papers have offset ω values derived from a *RadVel* analysis that are not included in Table 1. For instance, [Weiss et al. \(2017\)](#) meets all of

the criteria listed above, but the parameter set from [Weiss et al. \(2017\)](#) is not currently listed on the NASA Exoplanet Archive, so it was not flagged as reporting an incorrect ω value by our test. It is difficult to estimate how many papers were missed by our cross-referencing test, but we expect there to be several papers with offset ω values that are not included in Table 1. Thus, Table 1 is meant to serve as a guide for potential issues with ω values in the literature, not as a fully vetted list of all the papers and planetary systems that need their ω values corrected. However, it is clear that many ω values for the planets in Table 1 need to be updated as we strive to accurately elucidate the orbital geometries of planetary systems. This is especially relevant as we enter the age of combining archival RV data with astrometry (i.e. Gaia DR4) and direct imaging.

3. CONCLUSION

We find that **RadVel** yields ω_p rather than ω_* . As a result, we estimate that 265 published ω values in the literature are 180° offset from their true values. In future work, we encourage authors to be explicit in defining their coordinate system as well as if they are reporting ω_p or ω_* .

AH acknowledges support from the National Science Foundation REU Program (grant no. 2050527). AH

would like to thank Andrew Mayo and Greg Laughlin for several useful discussions. AH would also like to acknowledge the members of the AstroWeiss group for useful feedback on plotting. The authors would also like to thank the **RadVel** team for their feedback.

Software: **RadVel** (Fulton et al. 2018), **TTVFast** (Deck et al. 2014), **NumPy** (van der Walt et al. 2011), **Matplotlib** (Hunter 2007), **Pandas** (McKinney 2010)

REFERENCES

- Akeson, R. L., Chen, X., Ciardi, D., et al. 2013, *PASP*, 125, 989, doi: [10.1086/672273](https://doi.org/10.1086/672273)
- Deck, K. M., Agol, E., Holman, M. J., & Nesvorný, D. 2014, *ApJ*, 787, 132, doi: [10.1088/0004-637X/787/2/132](https://doi.org/10.1088/0004-637X/787/2/132)
- Foreman-Mackey, D., Hogg, D. W., Lang, D., & Goodman, J. 2013, *PASP*, 125, 306, doi: [10.1086/670067](https://doi.org/10.1086/670067)
- Fulton, B. J., Petigura, E. A., Blunt, S., & Sinukoff, E. 2018, *PASP*, 130, 044504, doi: [10.1088/1538-3873/aaaaa8](https://doi.org/10.1088/1538-3873/aaaaa8)
- Hunter, J. D. 2007, *Computing in Science and Engineering*, 9, 90, doi: [10.1109/MCSE.2007.55](https://doi.org/10.1109/MCSE.2007.55)
- Lovis, C., & Fischer, D. 2010, in *Exoplanets*, ed. S. Seager, 27–53
- McKinney, W. 2010, in *Proceedings of the 9th Python in Science Conference*, ed. S. van der Walt & J. Millman, 51 – 56
- Murray, C. D., & Correia, A. C. M. 2010, in *Exoplanets*, ed. S. Seager, 15–23
- Rosenthal, L. J., Fulton, B. J., Hirsch, L. A., et al. 2021, *ApJS*, 255, 8, doi: [10.3847/1538-4365/abe23c](https://doi.org/10.3847/1538-4365/abe23c)
- van der Walt, S., Colbert, S. C., & Varoquaux, G. 2011, *Computing in Science and Engineering*, 13, 22, doi: [10.1109/MCSE.2011.37](https://doi.org/10.1109/MCSE.2011.37)
- Weiss, L. M., Deck, K. M., Sinukoff, E., et al. 2017, *AJ*, 153, 265, doi: [10.3847/1538-3881/aa6c29](https://doi.org/10.3847/1538-3881/aa6c29)
- Wright, J. T., & Howard, A. W. 2013, *ApJS*, 205, 22, doi: [10.1088/0067-0049/205/2/22](https://doi.org/10.1088/0067-0049/205/2/22)
- Xuan, J. W., & Wyatt, M. C. 2020, *MNRAS*, 497, 2096, doi: [10.1093/mnras/staa2033](https://doi.org/10.1093/mnras/staa2033)

Table 1. A list of the papers affected by the argument of periastron issue in **RadVel**. For each paper, we include the corresponding host star as well as the number of planets with reported ω values affected by this issue.

Paper Reference	Host Star	Number of Affected Planets
Almenara et al. (2022)	GJ 3090	1
Almenara et al. (2022)	TOI-3884	1
Almenara et al. (2022)	WASP-148	2
Angelo et al. (2022)	Kepler-1656	2
Barnes et al. (2020)	DMPP-3 A	1
Barros et al. (2022)	HD 23472	5
Blunt et al. (2019)	HR 5183	1
Brady et al. (2018)	Kepler-1656	1
Brahm et al. (2019)	HD 1397	1
Brahm et al. (2020)	TOI-481	1
Cale et al. (2021)	AU MIC	1
Carleo et al. (2020)	TOI-421	2
Cointepas et al. (2021)	TOI-269	1
Dalba et al. (2020)	HD 332231	1
Dalba et al. (2022)	TOI-2180	1
Dedrick et al. (2021)	GJ 414 A	2
Demangeon et al. (2021)	HD 109286	1
Demangeon et al. (2021)	HD 115954	1
Demangeon et al. (2021)	HD 211403	1
Demangeon et al. (2021)	HD 27969	1
Demangeon et al. (2021)	HD 80869	1
Demangeon et al. (2021)	HD 95544	1
Demangeon et al. (2021)	L 98-59	4
Dragomir et al. (2019)	GJ 143	1
Fridlund et al. (2020)	TOI-763	2
Grieves et al. (2022)	TOI-5542	1
Hill et al. (2021)	iot Dra	2
Hobson et al. (2021)	TOI-201	1
Hurt et al. (2022)	GJ 411	2
Johnson et al. (2018)	K2-261	1
Kane et al. (2019)	HD 92987	1
Kane et al. (2019)	HD 221420b	1
Kanodia et al. (2020)	TOI-1728	1
Kawauchi et al. (2022)	TOI-2136	1
Kosiarek et al. (2019)	GJ 3470	1
Luque et al. (2021)	TOI-776	2

Table 1 *continued*

Table 1 (*continued*)

Paper Reference	Host Star	Number of Affected Planets
Luque et al. (2022)	HD 260655	2
Macdougall et al. (2021)	HIP 97166	2
Macdougall et al. (2022)	TOI-1272	2
Maldonado et al. (2021)	GJ 9689	1
Mawet et al. (2019)	eps Eri	1
Mills et al. (2019)	Kepler-68	1
Moutou et al. (2021)	TOI-1296	1
Moutou et al. (2021)	TOI-1298	1
Naponiello et al. (2022)	TOI-1422	1
Otegi et al. (2021)	TOI-1062	2
Piaulet et al. (2021)	WASP-107	2
Polanski et al. (2021)	Wolf 503	1
Robertson (2018)	YZ Cet	3
Rosenthal et al. (2021)	14 Her	2
Rosenthal et al. (2021)	16 Cyg B	1
Rosenthal et al. (2021)	47 UMa	3
Rosenthal et al. (2021)	51 Peg	1
Rosenthal et al. (2021)	55 Cnc	5
Rosenthal et al. (2021)	61 Vir	2
Rosenthal et al. (2021)	70 Vir	1
Rosenthal et al. (2021)	BD-10 3166	1
Rosenthal et al. (2021)	GJ 1148	2
Rosenthal et al. (2021)	GJ 15 A	1
Rosenthal et al. (2021)	GJ 179	1
Rosenthal et al. (2021)	GJ 317	2
Rosenthal et al. (2021)	GJ 411	2
Rosenthal et al. (2021)	GJ 414 A	2
Rosenthal et al. (2021)	GJ 436	1
Rosenthal et al. (2021)	GJ 581	2
Rosenthal et al. (2021)	GJ 649	1
Rosenthal et al. (2021)	GJ 687	1
Rosenthal et al. (2021)	GJ 849	2
Rosenthal et al. (2021)	GJ 876	3
Rosenthal et al. (2021)	HD 104067	1
Rosenthal et al. (2021)	HD 10697	1
Rosenthal et al. (2021)	HD 107148	2
Rosenthal et al. (2021)	HD 108874	2
Rosenthal et al. (2021)	HD 114729	1
Rosenthal et al. (2021)	HD 114783	2
Rosenthal et al. (2021)	HD 117207	1
Rosenthal et al. (2021)	HD 11964	2

Table 1 *continued*

Table 1 (*continued*)

Paper Reference	Host Star	Number of Affected Planets
Rosenthal et al. (2021)	HD 12661	2
Rosenthal et al. (2021)	HD 126614	1
Rosenthal et al. (2021)	HD 128311	1
Rosenthal et al. (2021)	HD 130322	1
Rosenthal et al. (2021)	HD 134987	2
Rosenthal et al. (2021)	HD 136925	1
Rosenthal et al. (2021)	HD 13931	1
Rosenthal et al. (2021)	HD 141004	1
Rosenthal et al. (2021)	HD 141399	4
Rosenthal et al. (2021)	HD 145934	1
Rosenthal et al. (2021)	HD 1461	2
Rosenthal et al. (2021)	HD 147379	1
Rosenthal et al. (2021)	HD 154345	1
Rosenthal et al. (2021)	HD 156279	2
Rosenthal et al. (2021)	HD 156668	2
Rosenthal et al. (2021)	HD 16141	1
Rosenthal et al. (2021)	HD 164922	4
Rosenthal et al. (2021)	HD 167042	1
Rosenthal et al. (2021)	HD 168009	1
Rosenthal et al. (2021)	HD 168443	2
Rosenthal et al. (2021)	HD 168746	1
Rosenthal et al. (2021)	HD 169830	2
Rosenthal et al. (2021)	HD 170469	1
Rosenthal et al. (2021)	HD 175541	1
Rosenthal et al. (2021)	HD 177830	2
Rosenthal et al. (2021)	HD 178911 B	1
Rosenthal et al. (2021)	HD 179949	1
Rosenthal et al. (2021)	HD 181234	1
Rosenthal et al. (2021)	HD 183263	2
Rosenthal et al. (2021)	HD 187123	2
Rosenthal et al. (2021)	HD 188015	1
Rosenthal et al. (2021)	HD 189733	1
Rosenthal et al. (2021)	HD 190360	2
Rosenthal et al. (2021)	HD 192263	1
Rosenthal et al. (2021)	HD 192310	1
Rosenthal et al. (2021)	HD 195019	1
Rosenthal et al. (2021)	HD 209458	1
Rosenthal et al. (2021)	HD 210277	1
Rosenthal et al. (2021)	HD 213472	1
Rosenthal et al. (2021)	HD 216520	1
Rosenthal et al. (2021)	HD 217107	2

Table 1 *continued*

Table 1 (*continued*)

Paper Reference	Host Star	Number of Affected Planets
Rosenthal et al. (2021)	HD 218566	1
Rosenthal et al. (2021)	HD 219134	6
Rosenthal et al. (2021)	HD 222582	1
Rosenthal et al. (2021)	HD 24040	2
Rosenthal et al. (2021)	HD 26161	1
Rosenthal et al. (2021)	HD 28185	1
Rosenthal et al. (2021)	HD 285968	1
Rosenthal et al. (2021)	HD 31253	1
Rosenthal et al. (2021)	HD 32963	1
Rosenthal et al. (2021)	HD 34445	1
Rosenthal et al. (2021)	HD 3651	1
Rosenthal et al. (2021)	HD 37124	3
Rosenthal et al. (2021)	HD 3765	1
Rosenthal et al. (2021)	HD 38529	2
Rosenthal et al. (2021)	HD 40979	1
Rosenthal et al. (2021)	HD 4203	2
Rosenthal et al. (2021)	HD 4208	1
Rosenthal et al. (2021)	HD 42618	1
Rosenthal et al. (2021)	HD 45184	2
Rosenthal et al. (2021)	HD 45350	1
Rosenthal et al. (2021)	HD 46375	1
Rosenthal et al. (2021)	HD 49674	1
Rosenthal et al. (2021)	HD 50499	2
Rosenthal et al. (2021)	HD 50554	1
Rosenthal et al. (2021)	HD 52265	1
Rosenthal et al. (2021)	HD 66428	2
Rosenthal et al. (2021)	HD 68988	2
Rosenthal et al. (2021)	HD 69830	3
Rosenthal et al. (2021)	HD 72659	1
Rosenthal et al. (2021)	HD 74156	2
Rosenthal et al. (2021)	HD 7924	3
Rosenthal et al. (2021)	HD 80606	1
Rosenthal et al. (2021)	HD 82943	2
Rosenthal et al. (2021)	HD 83443	1
Rosenthal et al. (2021)	HD 8574	1
Rosenthal et al. (2021)	HD 87883	1
Rosenthal et al. (2021)	HD 90156	1
Rosenthal et al. (2021)	HD 92788	2
Rosenthal et al. (2021)	HD 97658	1
Rosenthal et al. (2021)	HD 99109	1
Rosenthal et al. (2021)	HD 99492	1

Table 1 *continued*

Table 1 (*continued*)

Paper Reference	Host Star	Number of Affected Planets
Rosenthal et al. (2021)	HR 5183	1
Rosenthal et al. (2021)	eps Eri	1
Rosenthal et al. (2021)	rho CrB	2
Rosenthal et al. (2021)	tau Boo	1
Rosenthal et al. (2021)	ups And	3
Sarkis et al. (2018)	K2-18	1
Schlecker et al. (2020)	TIC 237913194	1
Sha et al. (2021)	TOI-954	1
Sha et al. (2021)	K2-329	1
Stefansson et al. 2020	K2-25	1
Stock et al. (2020)	GJ 251	1
Stock et al. (2020)	GJ 411	1
Stock et al. (2020)	HD 238090	1
Stock et al. (2020)	YZ Cet	2
Wilson et al. (2022)	TOI-1064	2
Yee et al. (2018)	HAT-P-11	2
Yu et al. (2018)	HD 89345	2
Yu et al. (2018)	K2-232	1
Zhang et al. (2021)	Kepler-129	1